Experimental study on the probability of inducing and detecting cavitation events in a soft solid

Gonzalo Garay
Laboratorio de Acústica Ultrasonora
Facultad de Ciencias
Montevideo, Uruguay
ggaray.uy@gmail.com

Yamil Abraham
Laboratorio de Acústica Ultrasonora
Facultad de Ciencias
Montevideo, Uruguay

Guillermo Cortela
Laboratorio de Acústica Ultrasonora
Facultad de Ciencias
Montevideo, Uruguay

Nicolás Benech
Laboratorio de Acústica Ultrasonora
Facultad de Ciencias
Montevideo, Uruguay

Carlos Negreira
Laboratorio de Acústica Ultrasonora
Facultad de Ciencias
Montevideo, Uruguay

2024 IEEE UFFC Latin America Ultrasonics Symposium (LAUS) | 979-8-3503-4908-5/24/$31.00 ©2024 IEEE | DOI: 10.1109/LAUS60931.2024.10552982

***Abstract*—The interaction between an intense ultrasonic field and a soft solid can generate bubbles that expand and collapse, known as acoustic cavitation. Understanding this phenomenon is crucial in controlling the formation of bubbles in specific brain areas during transcranial ultrasound therapies. To achieve this control, establishing an acoustic intensity threshold, beyond which cavitation is highly probable, becomes essential. As cavitation behavior can vary under identical experimental conditions, considering the probability of its occurrence becomes a crucial variable. This study introduces a passive detection system designed to identify acoustic cavitation, presenting the results of its implementation for a probabilistic analysis of cavitation phenomena. The setup comprises a high-power flat transducer operating at a frequency of 0.94 MHz, generating an acoustic field that traverses an agar-agar phantom. A secondary transducer, purpose-built for cavitation detection, captures the acoustic wave emitted by the phantom. The detection method involves analyzing the wave spectrum to identify the specific acoustic signature of bubbles: a subharmonic spectral component precisely at half the operating frequency. By conducting multiple iterations of the experiment, we determine how often cavitation is detected, thereby empirically establishing the likelihood of this phenomenon occurring. The results illustrate the correlation between the likelihood of cavitation occurrence and the maximum intensity of the applied acoustic field on the phantom. To elucidate the relationship between these variables, we introduce a model derived from calculating the effective volume where the acoustic field exceeds a threshold intensity value. This model aptly describes the experimental outcomes. Future work will extend this analysis to a transcranial HIFU experiment.**

***Index Terms*—Cavitation detection, HIFU.**

I. Introduction

Cavitation refers to the activity of a cloud of bubbles. This can be induced during the interaction of an intense ultrasonic field and a soft solid [1]. There are two regimes of cavitation that are not necessarily exclusive: transient cavitation and stable cavitation. When the bubble is induced, it grows following the cycles of compression and rarefaction of the ultrasound wave until it reaches a critical size. If after this, the bubble becomes unstable and collapses, we are facing transient cavitation. If, on the other hand, the bubble continues oscillating steadily for several cycles, we call it stable cavitation [2].

Understanding this phenomenon is crucial in controlling the formation of bubbles in specific brain areas during transcranial ultrasound therapies [3], [4]. To achieve this control, establishing an acoustic intensity threshold, beyond which cavitation is highly probable, becomes essential [4], [5]. As cavitation behavior can vary under identical experimental conditions, considering the probability of its occurrence becomes a crucial variable. The detection is based on the observation of the subharmonic frequency which appears during stable cavitation [6], [7].

The objective of this study is to implement a passive detection system designed to identify acoustic cavitation, define a criterion to identify the pressence of cavitation and model the probability of occurence or detection.

II. Method

The experimental setup is shown in Fig. 1. A flat transducer (Olympus) is employed as the emitter of ultrasonic waves to sonicate an agar-agar phantom. A passive cavitation detector (Sonic Concepts) receives the wave from the phantom. This system is submerged in degassed water to prevent cavitation generation outside the phantom.

The passive cavitation detector (PCD) is a flat transducer with a diameter $D_s = 23\,\mathrm{mm}$ and a nominal frequency of 2 MHz. Its nominal -3 dB bandwidth is 48%, and its -20 dB bandwidth is 139%. The size of its surface and the wide bandwidth make it sensitive to a wide range of frequencies, particularly to the low-intensity frequencies generated by cavitation. The PCD is positioned in a confocal arrangement at a distance $L = 88\,\mathrm{mm}$ from the focal point. The acquired signal is digitized on the oscilloscope (OSC) and stored on the computer (PC).

The transmitting transducer is a flat single-element with a nominal diameter $D = 28.575\,\mathrm{mm}$ (1.125 inches) and

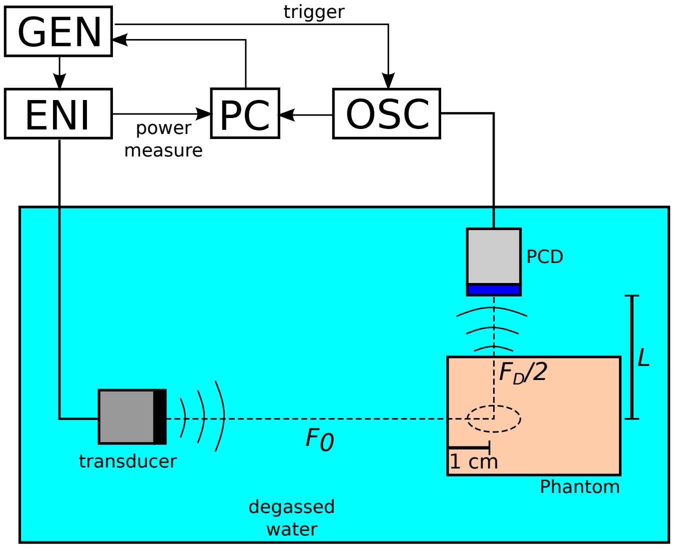

Fig. 1. Experimental setup. A flat transducer sonicates an agar-agar phantom. The PCD receives the wave from the phantom. This system is submerged in degassed water.

a nominal frequency of 1 MHz. Manufacturer characterization indicates that the central frequency of the transducer, at which maximum amplitude is detected in its spectrum, is $f_0 = 0.94\,\mathrm{MHz}$. In this experiment, we will operate at this frequency to optimize power transmission through the transducer.

The phantom is a cylindrical sample (diameter 60 mm, height 70 mm) of a solidified solution (1.75% w/v) of agar-agar powder and water [8]. It was characterized by measuring its density ρ, longitudinal wavespeed c, attenuation coefficient α at 1 MHz, and the nonlinear parameter B/A. These parameters was measured relatively to water parameters assumed from refs. [9], [10], [11] and [12]. Density was measured through a hydrostatic weighing. The longitudinal wavespeed and the attenuation coefficient was measured through ultrasonic transmission by measuring the time of flight and the amplitude attenuation [13]. The B/A parameter was measured by a finite amplitude insert-substitution method (FAIS) [12]. The parameters are summarized in Table I. In the experiment, the phantom is positioned in such a way that the wave impacts one of its flat faces, and the focal point is located 1 cm inside.

In the experiment, the transmitting transducer is excited with a function generator (Tektronix AFG 3021B) magnified by a power amplifier with a gain of 50 dB (E&I A075). The signal consists of a sine function with a frequency $f_0 = 0.94\,\mathrm{MHz}$, duration $705\,\mu\mathrm{s}$, and amplitude ranging from $V_{in} = 32\,\mathrm{V}$ to

TABLE I
WAVE PROPAGATION PROPERTIES AT 20°C AND 1 MHz.

	ρ (g/cm^3)	c (mm/μs)	α (dB/cm)	B/A
water[a]	0.998	1.485	0.0022	5.2
phantom	1.001	1.489	0.0292	7.2

[a]From refs. [9], [10], [11] and [12].

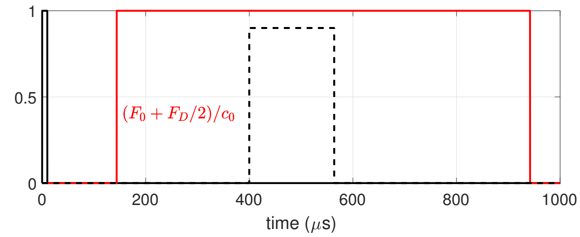

Fig. 2. Ultrasound sequence scheme used for cavitation generation and detection. At $t = 0$, the wave is emitted from the transducer. The red line represents the time window during which the ultrasonic signal scattered from the phantom is expected to be received at the PCD. The dashed line represents the time window during which the acquisition takes place.

$V_{in} = 158\,\mathrm{V}$. Fig. 2 schematically illustrates the emission-acquisition sequence. At $t = 0$, the wave is emitted. If c_0 is the propagation velocity in water, it is estimated that the wave arriving from the focus will arrive at $t = (F_0 + F_D/2)/c_0$, where F_0 is the focal distance of the transmitting transducer and F_D is the focal distance of the PCD. In the configuration, the PCD is placed at a distance $F_D/2$ from the focal point of the transmitting transducer (Fig. 1). The time window in which this signal is expected to be received is shown in red. The acquisition window, indicated by the dashed line, begins at $t = 400\,\mu\mathrm{s}$ and lasts for $164\,\mu\mathrm{s}$. This ensures that the acquisition occurs away from the wave's arrival and far from its end, avoiding transient regimes that occur at the beginning and end of the signal. Additionally, the signal duration is sufficient to encompass multiple cycles of the received signal and allows for several acquisitions without saturating the oscilloscope's memory. With these parameters, the emission-acquisition sequence is repeated 768 times for each voltage employed.

III. Results

The signal analysis is performed through the analysis of their spectra. Fig. 3 display the spectra of two signals measured with the same voltage ($V_{in} = 158\,\mathrm{V}$), the maximum used in the experiment.

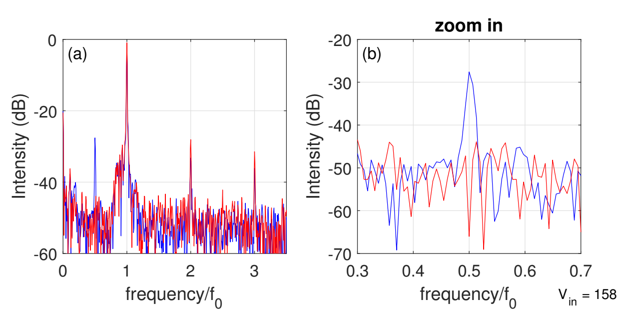

Fig. 3. (a) Spectra corresponding to the signals acquired in shots 70 (blue) and 92 (red) measured with an applied voltage $V_{in} = 158\,\mathrm{V}$ (b) Enlargement of the spectra around the frequency of the subharmonic. The frequency scale is normalized to easily recognize the fundamental frequency ($f/f_0 = 1$) and the subharmonic frequency ($f/f_0 = 0.5$).

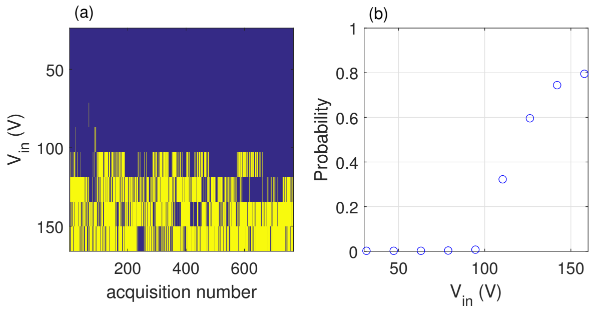

Fig. 4. (a) Detection scheme. A yellow line indicates for each voltage at which acquisition number a positive detection was obtained. (b) Probability calculated for each voltage by dividing the number of positive detections by the total number of acquisitions.

Both spectra in Fig. 3 correspond to different sonications and were chosen based on the difference they show. In one case, we can observe the frequency of the first subharmonic (blue line). In the other case, the intensity remains at the level of noise (red line). This shows that with the same applied voltage, the detection of cavitation is associated with a probability function.

To determine the probability function, we must first establish a criterion to define a positive detection. For this, we will set a threshold intensity level that must be reached at the subharmonic frequency to be above the noise level. This threshold value is -43 dB.

Probability is calculated for each applied voltage by dividing the number of signals where a cavitation event was detected by the total number of acquisitions. The image on Fig. 4(a) shows in yellow the acquisitions where there was a positive detection and in blue the acquisitions where there was not. The calculation of probability is shown in Fig. 4(b) as a function of the applied voltage.

The physical model for determining the probability of occurrence and detection of cavitation is based on defining a region where the phenomenon can occur and be detected. Additionally, it requires a threshold intensity above which the phenomenon occurs. First, we define a volume that satisfies two conditions: (1) cavitation has a high probability of occurring; (2) cavitation has a high probability of being detected.

The simplest approach is to define this region as a cylinder whose geometric center is at the focus of the transducer and whose flat faces are perpendicular to the detector beam. This

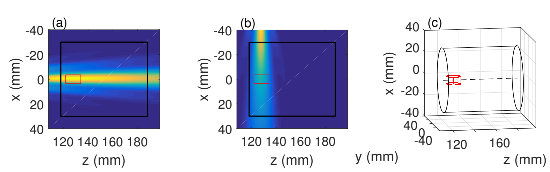

Fig. 5. (a) Cross-sectional view of the transducer's acoustic field, the phantom volume (black line), and the volume defined where cavitation is highly likely to occur (red line). (b) Detector's acoustic field. (c) Three-dimensional representation of defined volume, included within the edges of the phantom.

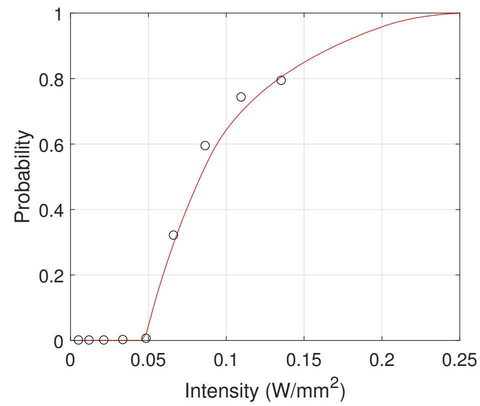

Fig. 6. Probability curve of cavitation detection/occurrence. Circles represent experimental data. The red line represents the physical model.

configuration is shown in Fig. 5. The red lines represent the edges of the cylinder we have defined, and the black lines represent the edges of the phantom. Fig. 5(a) depicts a cross-sectional view of the transducer's acoustic field and the mentioned volume. We consider that the region where cavitation has a high probability of occurring is within the focal width of the transducer. This is defined as the area where the acoustic intensity decreases to half of the intensity at the focal point. Fig. 5(b) shows the acoustic field calculated for the detector. Considering the reciprocity in the emission and reception of a transducer, the region where cavitation is most likely to be detected (if generated) is limited by the width of the detector's beam. This width is defined similarly to the focal width.

Having defined this cylinder, we proceed to define a threshold intensity such that, if this acoustic intensity is exceeded within the cylinder, cavitation will occur. Assuming that the transducer's field obeys a piston mode, we can calculate the volume included in the cylinder where the intensity exceeds the threshold value. Our strongest hypothesis is that the probability of generating and detecting cavitation is proportional to the mentioned volume. Therefore, we propose to calculate the probability as the ratio between this volume and the total volume of the cylinder defined previously. The final result is shown in Fig. 6 as a function of the ultrasonic intensity. The circles shows the experimental probability and the red line the probability computed from the model. The presented model predicts well the behavior of the probability determined experimentally.

IV. Final Remarks

It was presented a model that predicts the behavior of the probability curve of detect or generate cavitation. However, the model and the experiment are not independent since the threshold intensity is a characteristic parameter of the model but is determined from experimental data. For this reason, this study (experiment and model) can function as a method of characterizing the phantom, given that this parameter was introduced as a characteristic of the medium in which cavitation occurs. In future works, this study will be applied to different kind of phantoms and the thermal behavior will be analyzed.

REFERENCES

[1] C. E. Brennen, “Cavitation in medicine,” *Interface focus*, vol. 5, no. 5, p. 20150022, 2015.

[2] Z. Izadifar, P. Babyn, and D. Chapman, “Ultrasound cavitation/microbubble detection and medical applications,” *Journal of Medical and Biological Engineering*, vol. 39, pp. 259–276, 2019.

[3] G. Maimbourg, A. Houdouin, M. Santin, S. Lehericy, M. Tanter, and J.-F. Aubry, “Inside/outside the brain binary cavitation localization based on the lowpass filter effect of the skull on the harmonic content: a proof of concept study,” *Physics in Medicine & Biology*, vol. 63, no. 13, p. 135012, 2018.

[4] Y.-S. Tung, F. Vlachos, J. J. Choi, T. Deffieux, K. Selert, and E. E. Konofagou, “In vivo transcranial cavitation threshold detection during ultrasound-induced blood–brain barrier opening in mice,” *Physics in Medicine & Biology*, vol. 55, no. 20, p. 6141, 2010.

[5] A. Coleman, T. Kodama, M. Choi, T. Adams, and J. Saunders, “The cavitation threshold of human tissue exposed to 0.2-mhz pulsed ultrasound: Preliminary measurements based on a study of clinical lithotripsy,” *Ultrasound in medicine & biology*, vol. 21, no. 3, pp. 405–417, 1995.

[6] W. Lauterborn, “Numerical investigation of nonlinear oscillations of gas bubbles in liquids,” *The Journal of the Acoustical Society of America*, vol. 59, no. 2, pp. 283–293, 1976.

[7] V. Ilyichev, V. Koretz, and N. Melnikov, “Spectral characteristics of acoustic cavitation,” *Ultrasonics*, vol. 27, no. 6, pp. 357–361, 1989.

[8] S. Daniels, D. Blondel, L. Crum, G. Ter Haar, and M. Dyson, “Ultrasonically induced gas bubble production in agar based gels: Part i, experimental investigation,” *Ultrasound in medicine & biology*, vol. 13, no. 9, pp. 527–539, 1987.

[9] P. Bigg, “Density of water in si units over the range 0-40 c,” *British Journal of Applied Physics*, vol. 18, no. 4, p. 521, 1967.

[10] V. Del Grosso and C. Mader, “Speed of sound in pure water,” *the Journal of the Acoustical Society of America*, vol. 52, no. 5B, pp. 1442–1446, 1972.

[11] J. Pinkerton, “A pulse method for the measurement of ultrasonic absorption in liquids: results for water,” *Nature*, vol. 160, no. 4056, pp. 128–129, 1947.

[12] X.-f. Gong, Z.-m. Zhu, T. Shi, and J.-h. Huang, “Determination of the acoustic nonlinearity parameter in biological media using fais and itd methods,” *The Journal of the Acoustical Society of America*, vol. 86, no. 1, pp. 1–5, 1989.

[13] G. A. Cortela, C. A. Negreira, and W. C. Pereira, “Durability study of a gellan gum-based tissue-mimicking phantom for ultrasonic thermal therapy,” *The Journal of the Acoustical Society of America*, vol. 147, no. 3, pp. 1531–1545, 2020.